Supplementary Figure 1

Sait Ozturk et al.

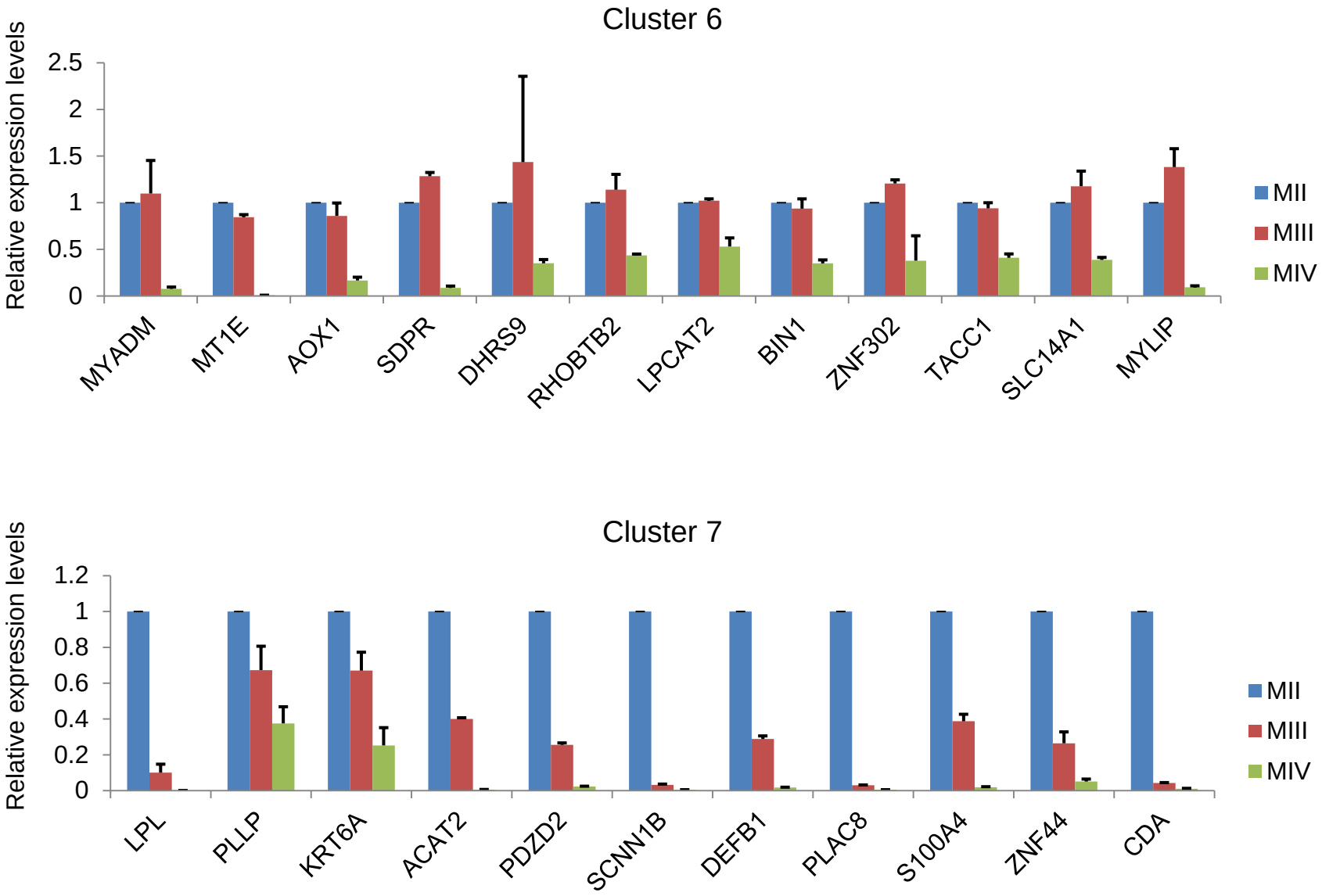

Supplementary Figure 1: Expression of candidate metastasis suppressor genes. The graphs show the mRNA levels of candidate metastasis suppressor genes among the breast cancer progression model cell lines. Following meta-analysis on Oncomine™ and quantitative RT-PCR, our list consist of 23 genes, 12 genes from cluster 6 and 11 from cluster 7.

Supplementary Figure 2

Sait Ozturk et al.

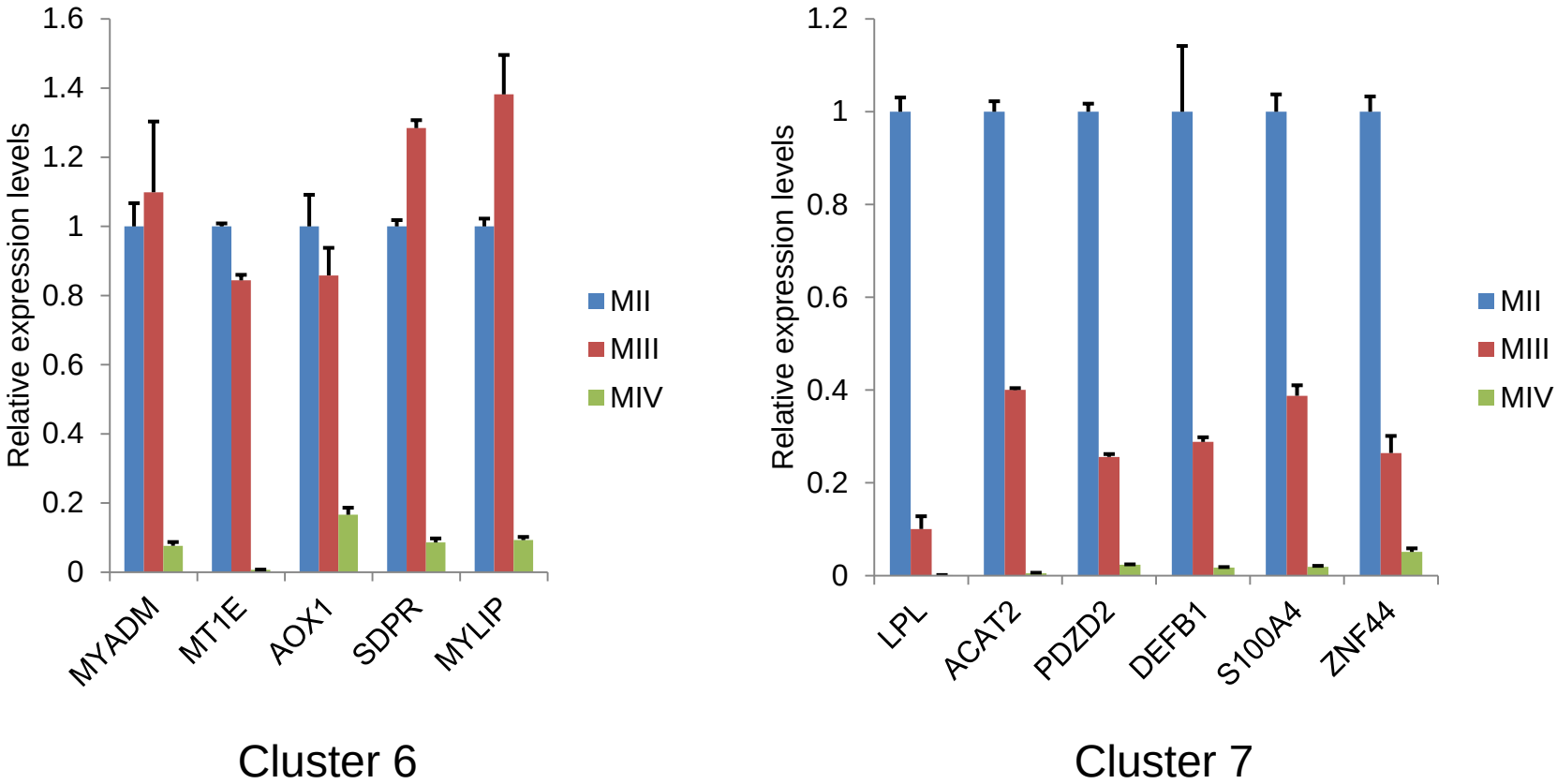

Supplementary Figure 2: The eleven major candidate genes. To increase the stringency of our filtering process on candidate genes, we set the requirement for the mRNA expression difference between each model cell line to be at least three fold. These led to exclusion of 12 genes from the 23 and resulted in 11 major candidate metastasis suppressor genes. All of these eleven genes are significantly repressed in metastatic MIV cells compared to the pre-malignant, MII and pre-metastatic, MIII cells.

Supplementary Figure 3

Sait Ozturk et al.

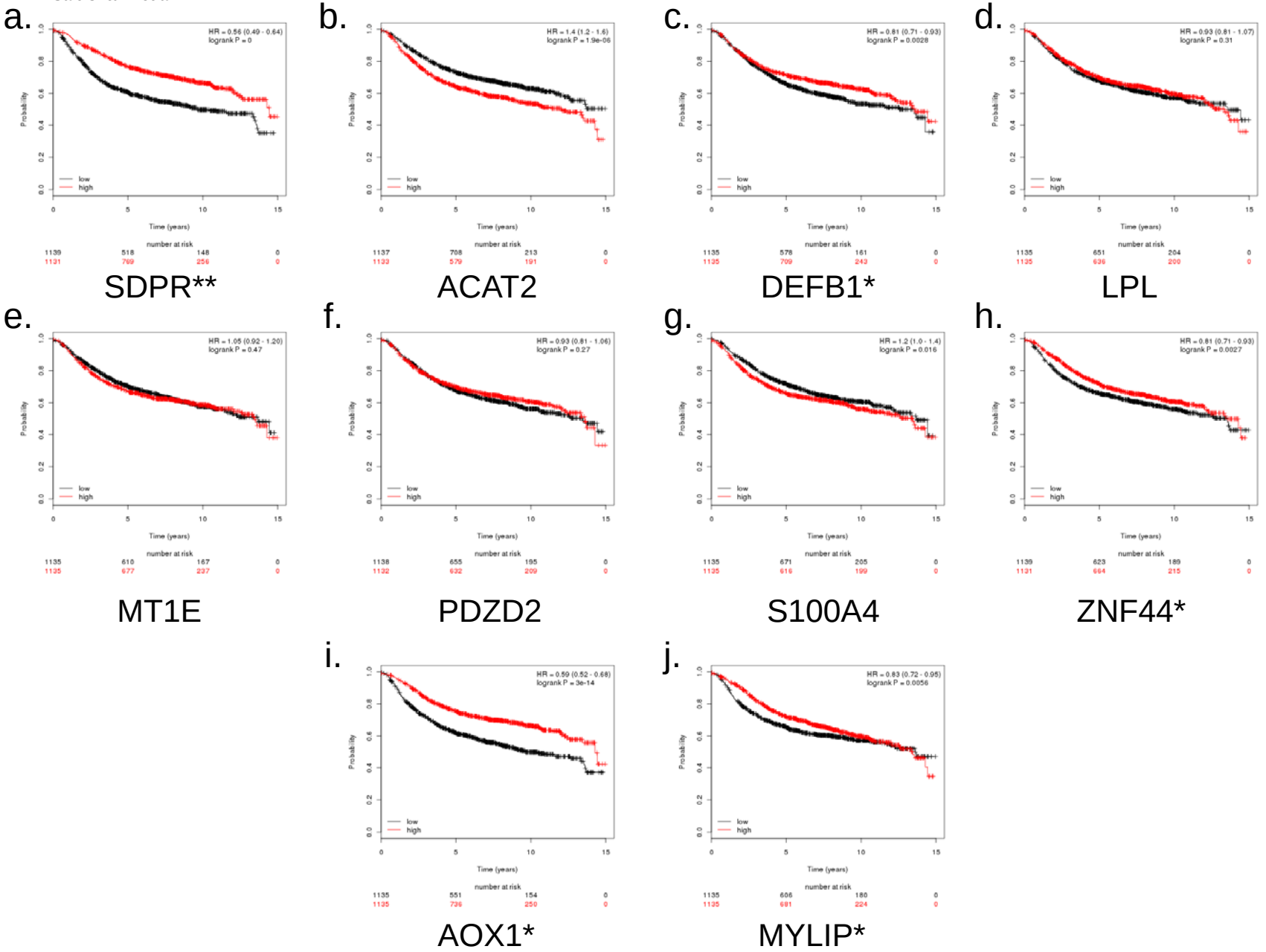

Supplementary Figure 3: Relapse-free survival curves based on candidate metastasis suppressor gene expression. Kaplan-Meier plots were generated by the online software tool, Kaplan-Meier Plotter. The patient cohort was split into two groups, high (red line) and low (black line) based on the median expression levels of the gene in query. Among the candidate metastasis suppressor genes, expression of *SDPR* **(a)**, *DEFB1* **(g)**, *ZNF44* **(h)**, *AOX1* **(i)** and *MYLIP* **(j)** were associated with an increased relapse-free survival probability. Among these five genes *SDPR* exhibited the lowest *p*-value. A Kaplan-Meier plot could not be generated for *MYADM* because the probe was not represented in the database at the time of analysis.

Supplementary Figure 4

Sait Ozturk et al.

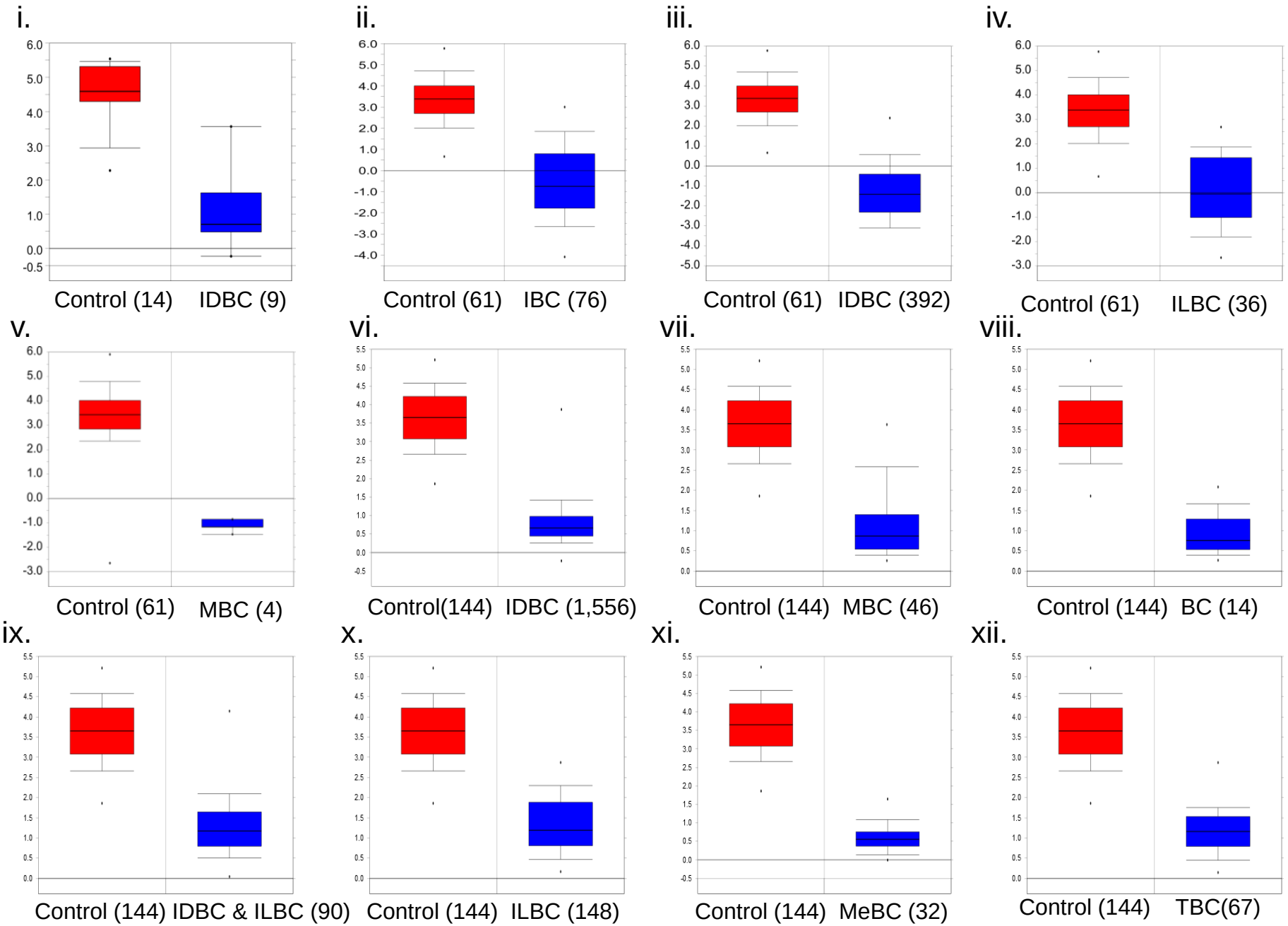

Supplementary Figure 4: Expression of SDPR in clinical samples. 12 gene expression profiling studies from the Oncomine™ database showing SDPR expression in breast cancer. IDBC: Invasive Ductal Breast Carcinoma, IBC: Invasive Breast Carcinoma, ILBC: Invasive Lobular Breast Carcinoma, MBC: Mucinous Breast Carcinoma, BC: Breast Carcinoma, MeBC: Medullary Breast Carcinoma, TBC: Tubular Breast Carcinoma. *p*-values are: i. 5.95E-07, ii. 3.70E-33, iii. 2.32E-14, iv. 2.68E-55, v. 1.16E-17, vi. 4.64E-81 **vii.** 6.55E-64, viii. 3.28E-56, xi. 3.45E-63, x. 6.27E-90, xi. 1.73E-31 and xii. 1.35E-13. Numbers in parenthesis indicate the sample sizes. (1-3)

Supplementary Figure 5

Sait Ozturk et al.

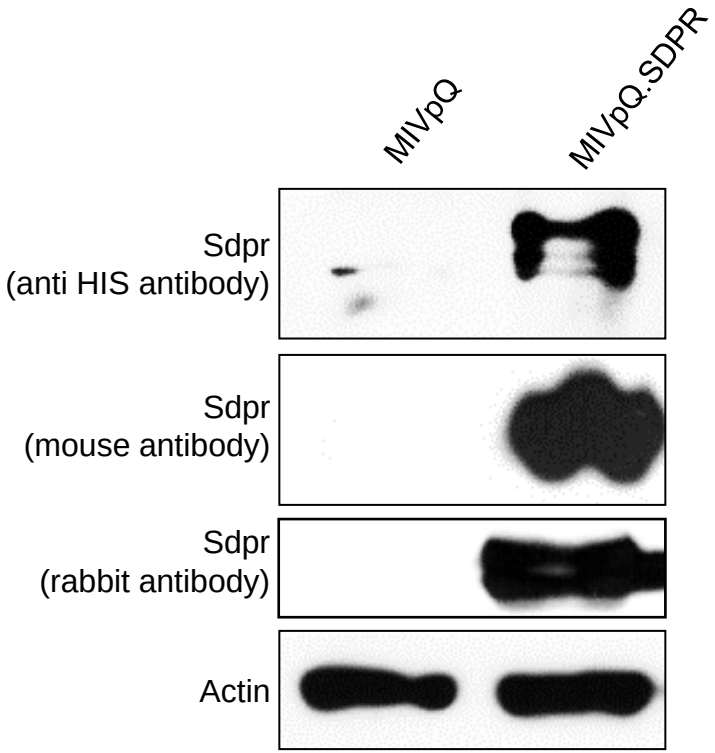

Supplementary Figure 5: SDPR overexpression in MIV cells. Detection of His-tagged SDPR expression was performed by Western blotting with three separate antibodies.

Supplementary Figure 6

Sait Ozturk et al.

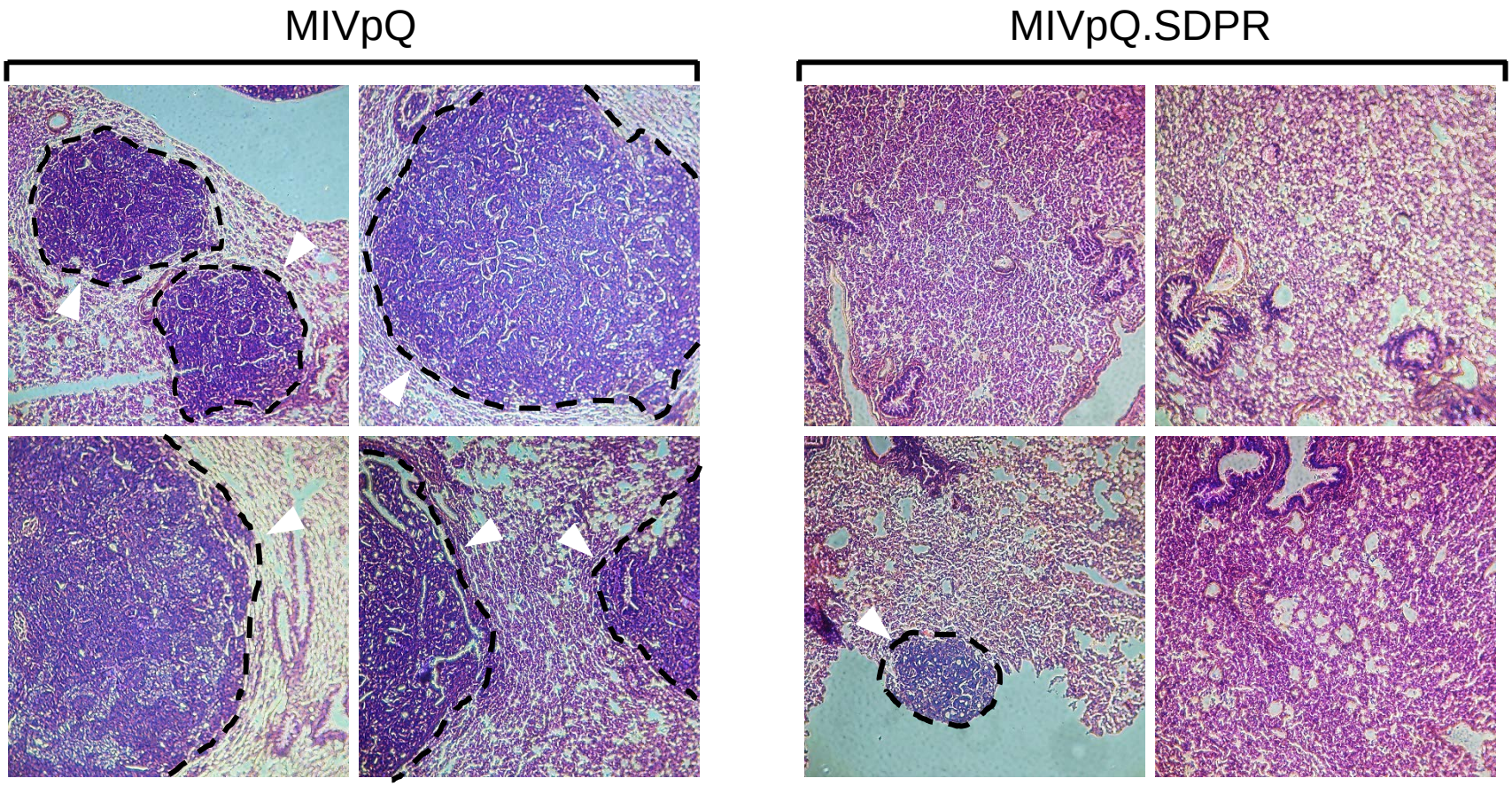

Supplementary Figure 6: SDPR overexpression inhibits lung colonization. Hematoxylin and eosin staining was done on lungs isolated from the indicated animals. Pictures show representative H&E stained slides, metastases are highlighted.

Supplementary Figure 7

Sait Ozturk et al.

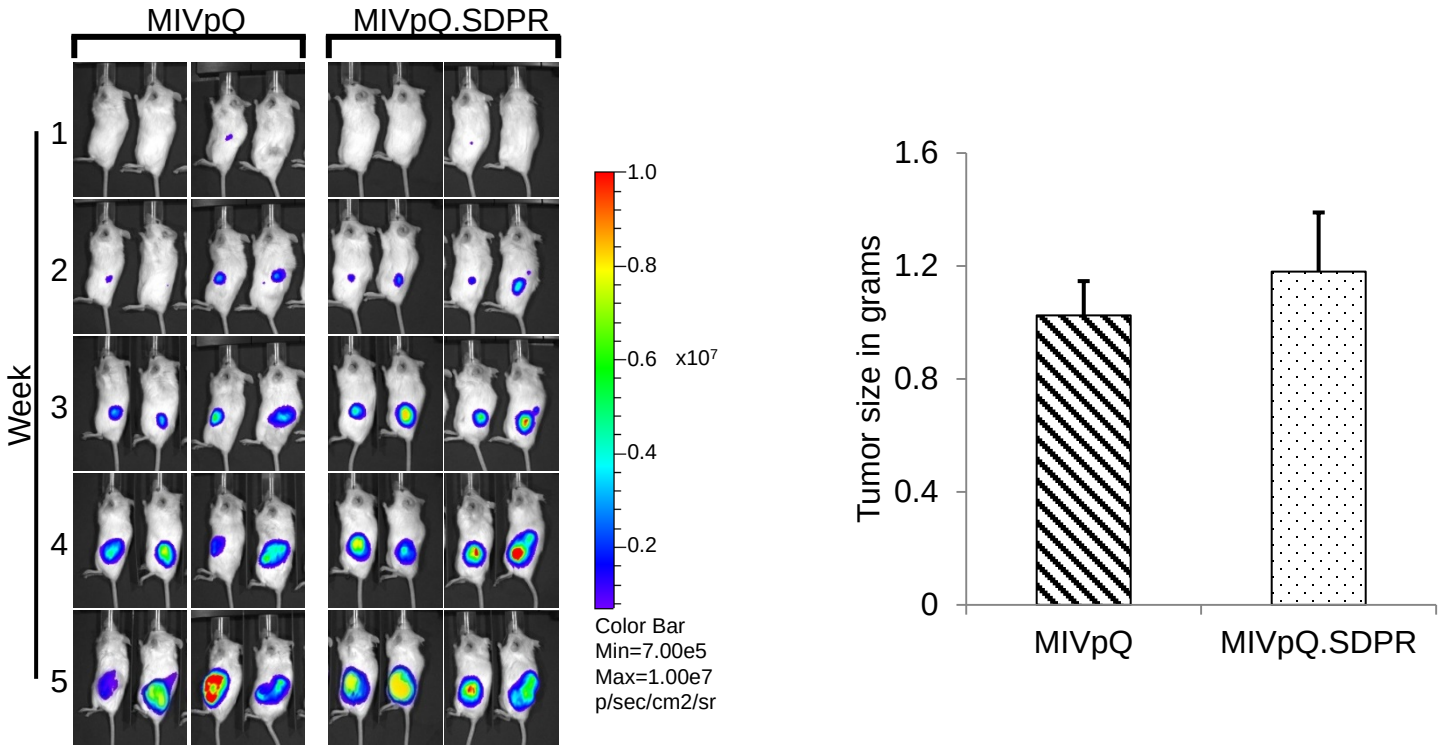

Supplementary Figure 7: SDPR does not affect primary tumor growth. Control (MIVpQ) and SDPR overexpressing (MIVpQ.SDPR) cells were injected subcutaneously, and tumor growth was tracked using bioluminescent imaging for five weeks (left panel). At the end of the experiment tumors were extracted and weighed (right panel).

Supplementary Figure 8

Sait Ozturk et al.

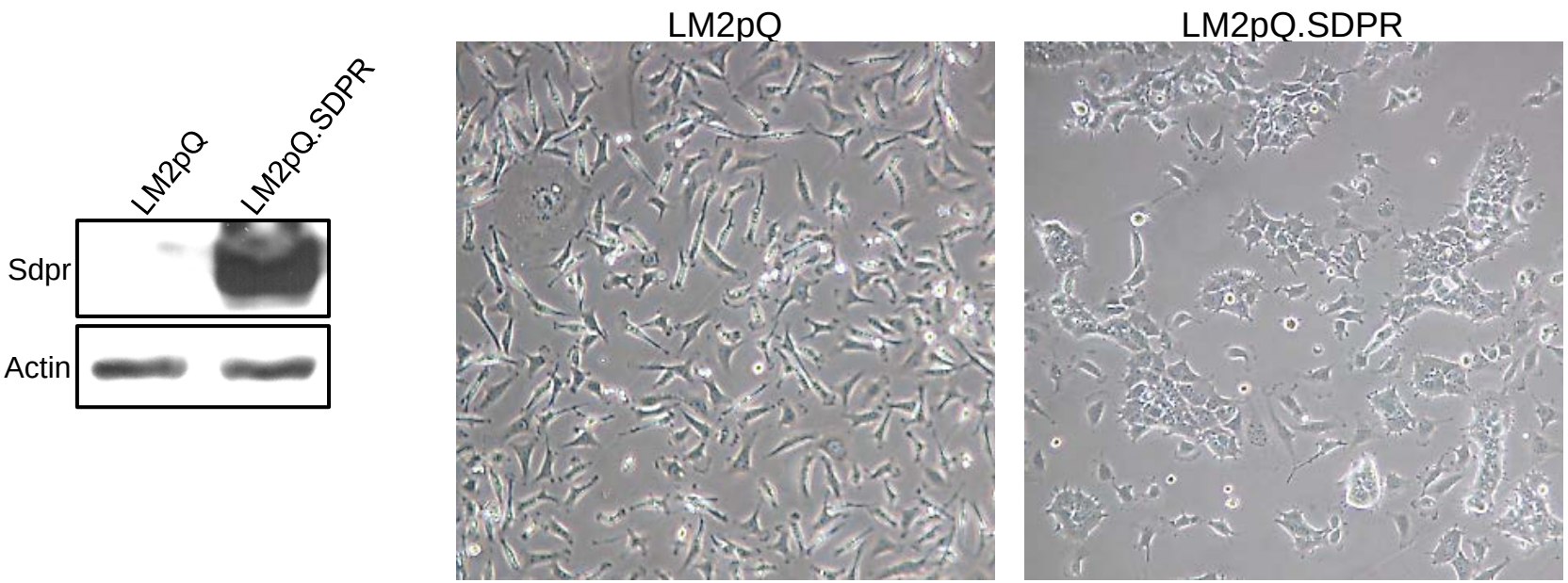

Supplementary Figure 8: SDPR expression alters the cell morphology of LM2. Western blot depicting SDPR overexpression in LM2 cells is on the left and light microscopy showing the more epithelial-like morphology of SDPR-expressing LM2 cells is on the right panel.

Supplementary Figure 9

Sait Ozturk et al.

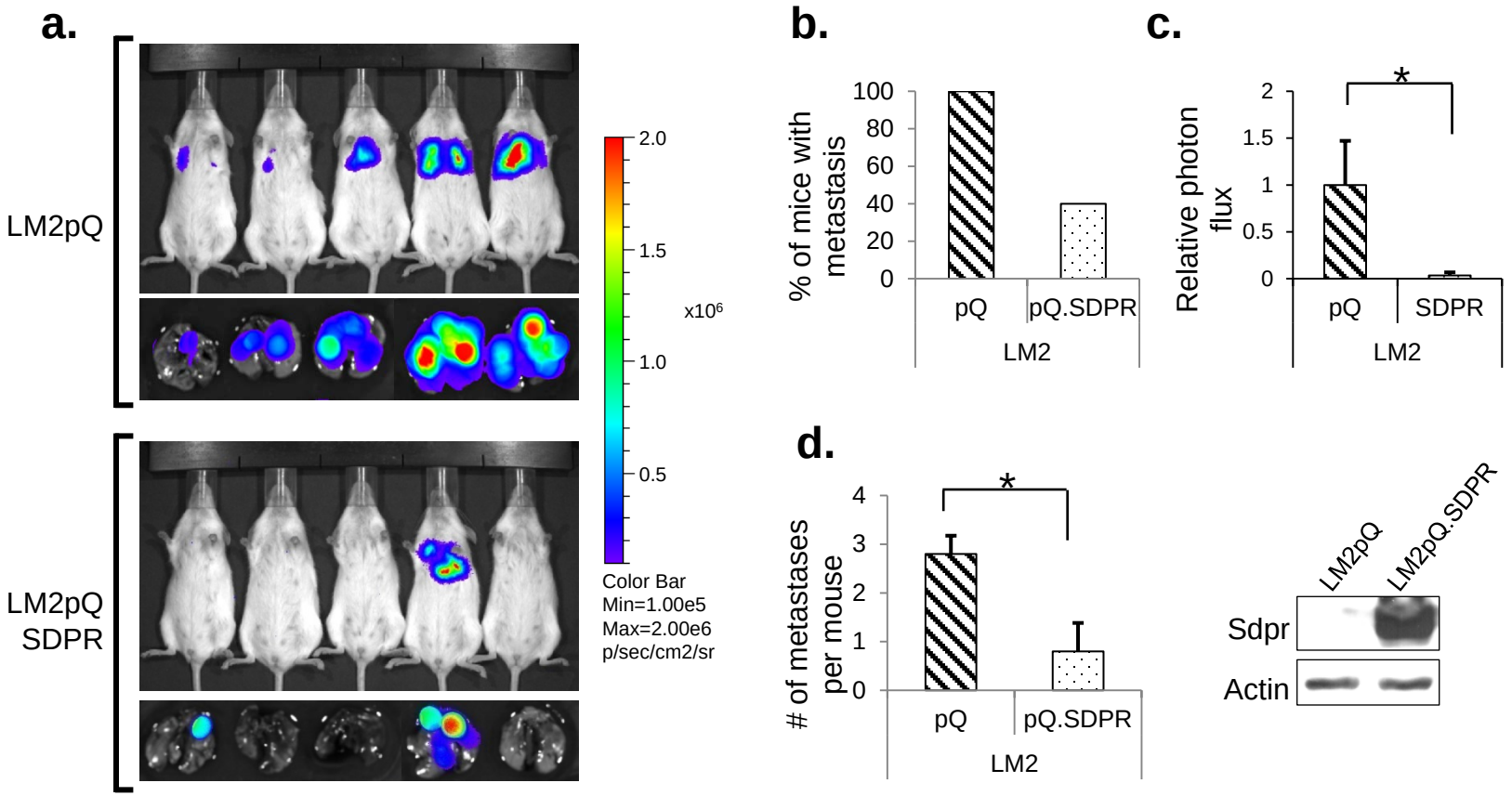

Supplementary Figure 9: SDPR suppresses lung colonization of breast cancer. (a) Bioluminescent imaging of animals 35 days after tail vein injections with $5x10^5$ control or LM2pQ.SDPR cells. **(b)** The percentage of animals that developed lung metastases following the tail vein injections with control or LM2pQ.SDPR cells is shown. **(c)** The quantification of metastases burden on mice was done by photon flux measurement, p=0.037. **(d)** The average number of lung macrometastases observed per animal upon injection with control or LM2pQ.SDPR cells**,** p=0.006. * indicates P<0.05.

Supplementary Figure 10

Sait Ozturk et al.

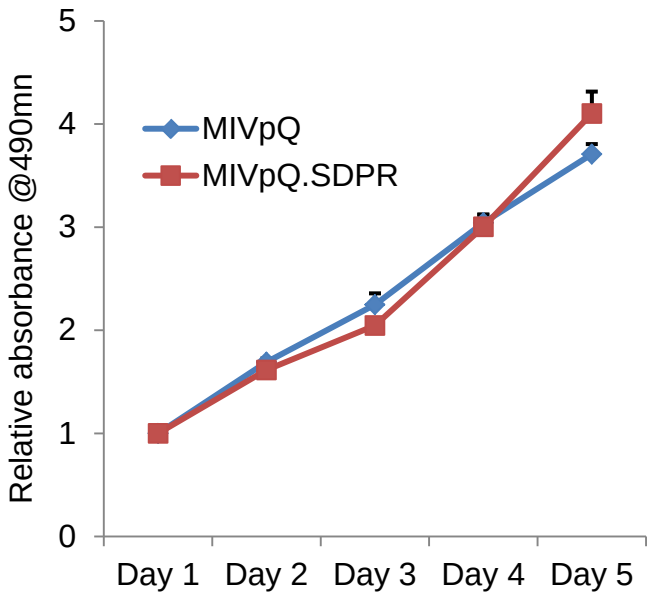

Supplementary Figure 10: SDPR expression does not affect cell proliferation. SDPR overexpression in MIV cells did not affect cell proliferation as measured by MTS tetrazolium/PMS assay.

Supplementary Figure 11

Sait Ozturk et al.

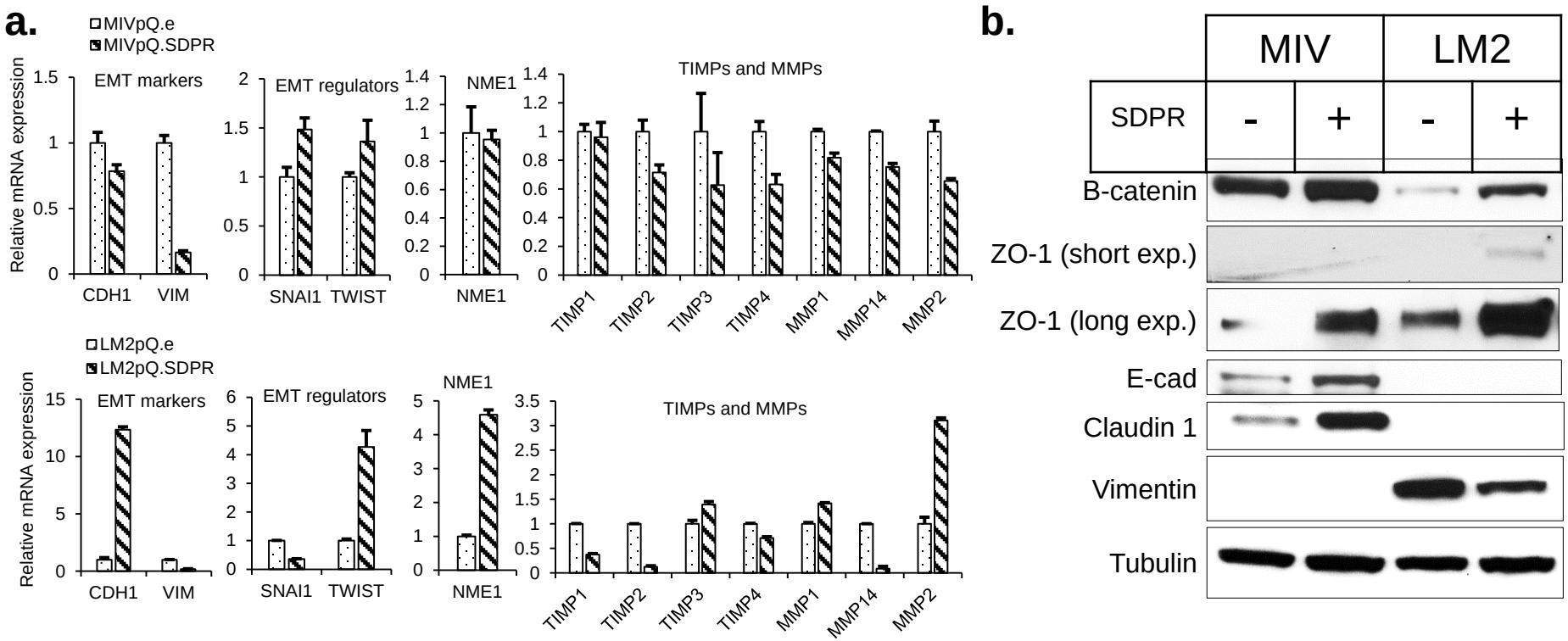

Supplementary Figure 11: Effect of SDPR on genes involved in EMT and metastasis. (a) Q-RT-PCR was performed to assess the transcript levels of known EMT and metastasis related genes upon SDPR overexpression. (b) Western blot analysis was performed to observe the changes on EMT protein markers following SDPR overexpression in MIV and LM2 cells.

Supplementary Figure 12

Sait Ozturk et al.

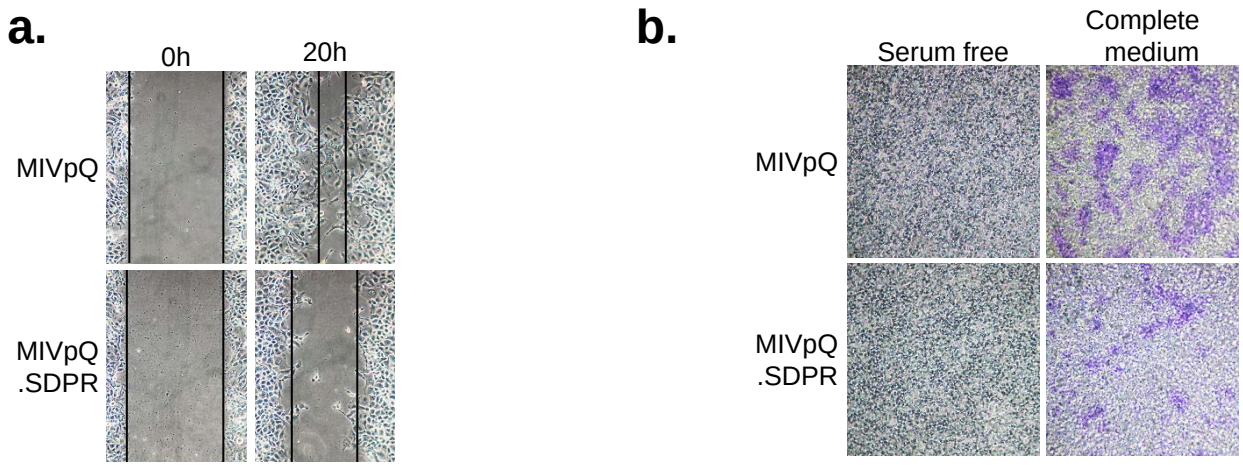

Supplementary Figure 12: SDPR impairs cell migration. (a) SDPR overexpression in MIV cells caused a slower rate of migration in scratch wound healing assay. **(b)** Boyden chamber migration assay revealed that fewer cells migrated through the membrane with 8 micron pores upon SDPR overexpression.

Supplementary Figure 13

Sait Ozturk et al.

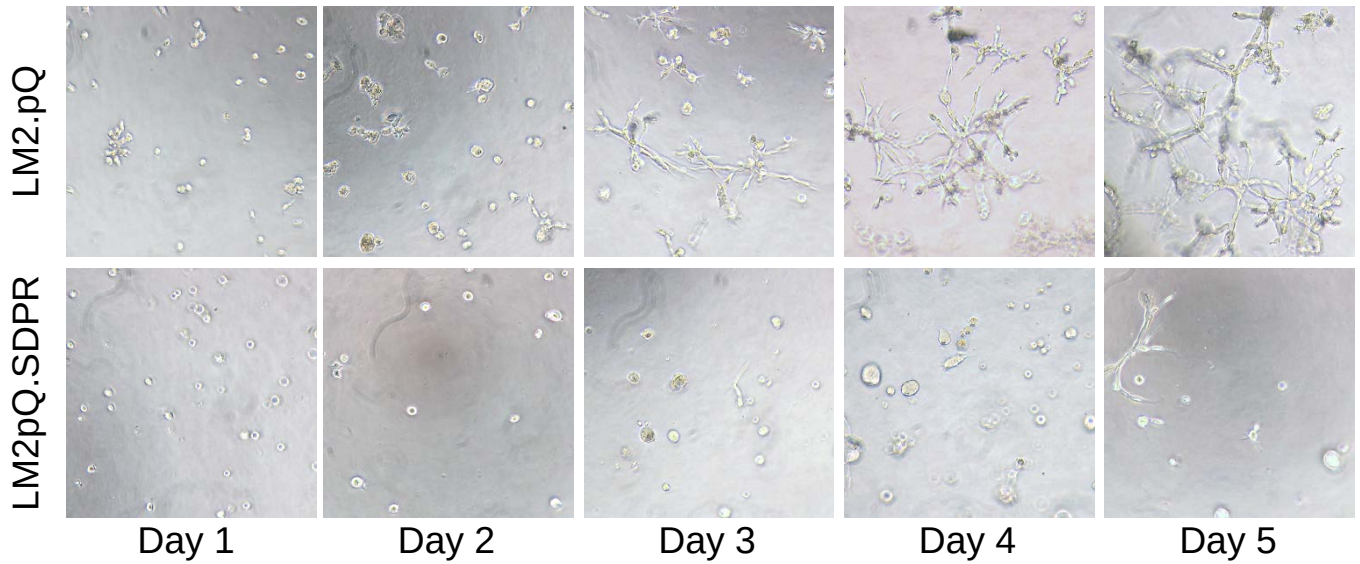

Supplementary Figure 13: SDPR blocks cell growth upon loss of adhesion. The effect of SDPR overexpression on the growth of LM2 cells in 3D cell culture was assessed for 5 days.

Supplementary Figure 14

Sait Ozturk et al.

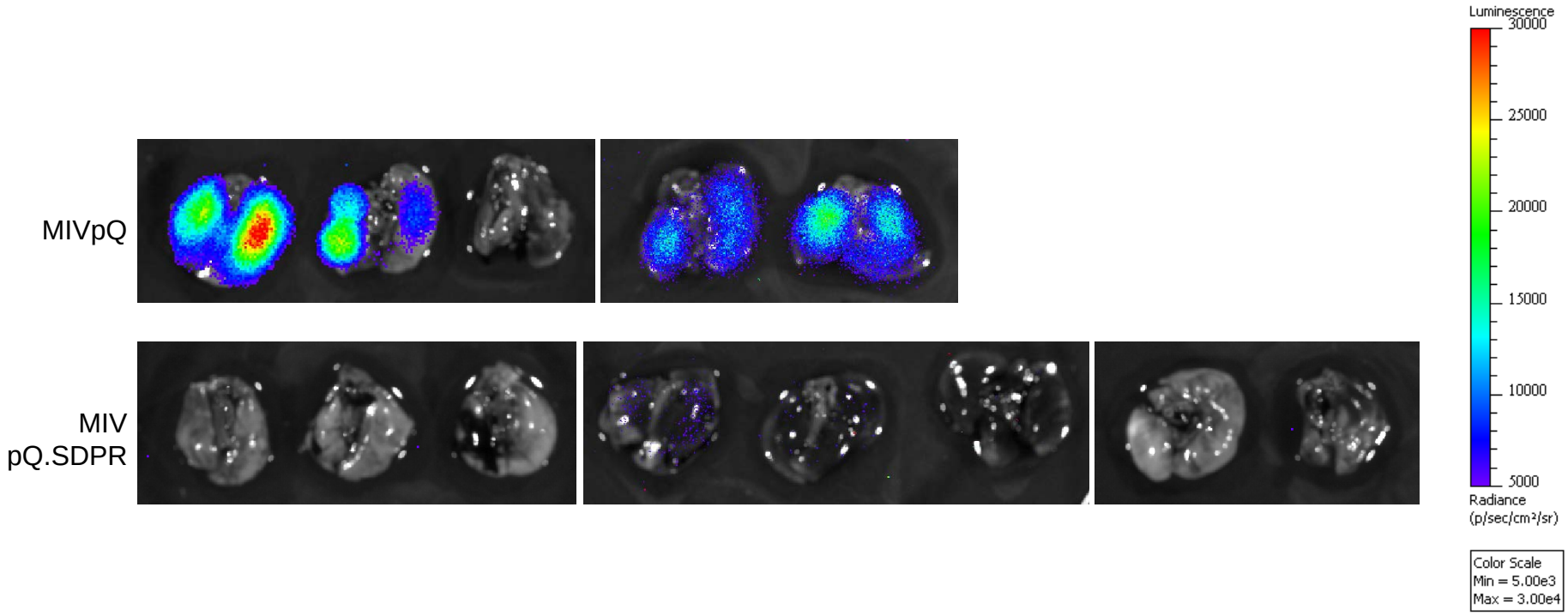

Supplementary Figure 14: Lung colonization assay. Nod/SCID mice were injected with $5x10^5$ MIVpQ or MIVpQ.SDPR cells through the tail vein. 72 hour post injection, lungs are extracted and imaged to assess the number of cells surviving.

Supplementary Figure 15

Sait Ozturk et al.

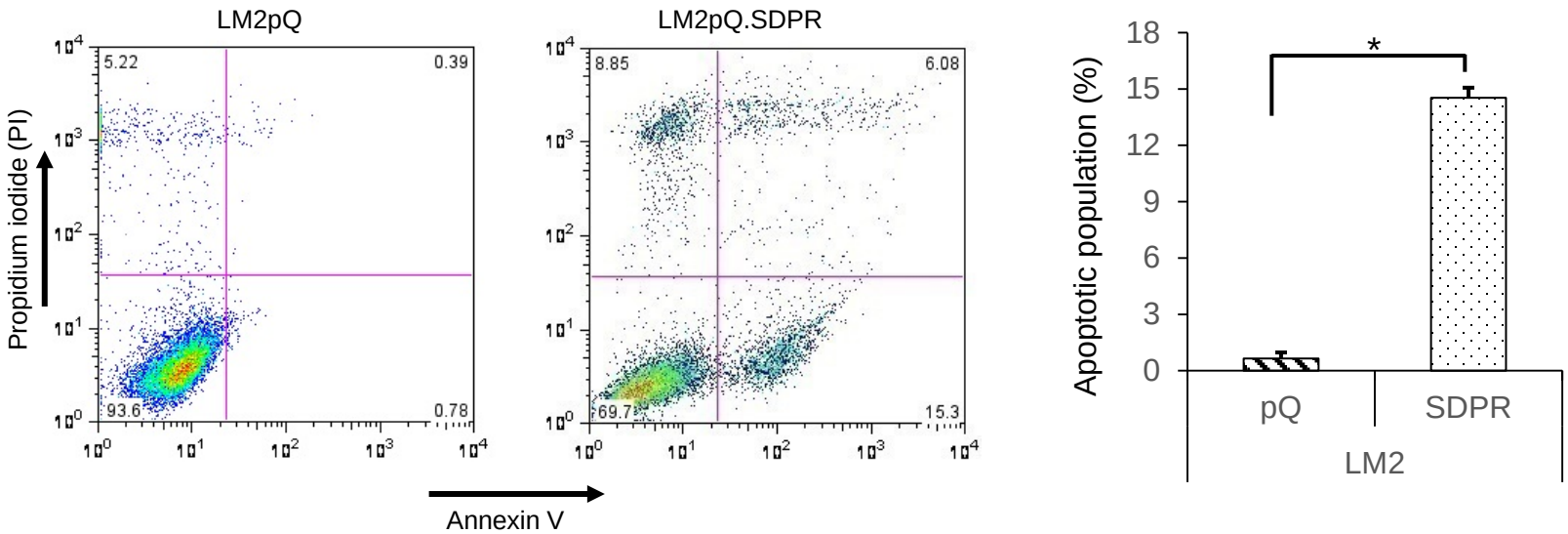

Supplementary Figure 15: SDPR overexpression promotes the apoptotic population in LM2 cells. Annexin V and propidium iodide staining were used to assess the basal level of apoptosis in control *versus* LM2pQSDPR cells; quantification of three independent experiments is shown, p=0.0001. * indicates P<0.05.

Supplementary Figure 16

Sait Ozturk et al.

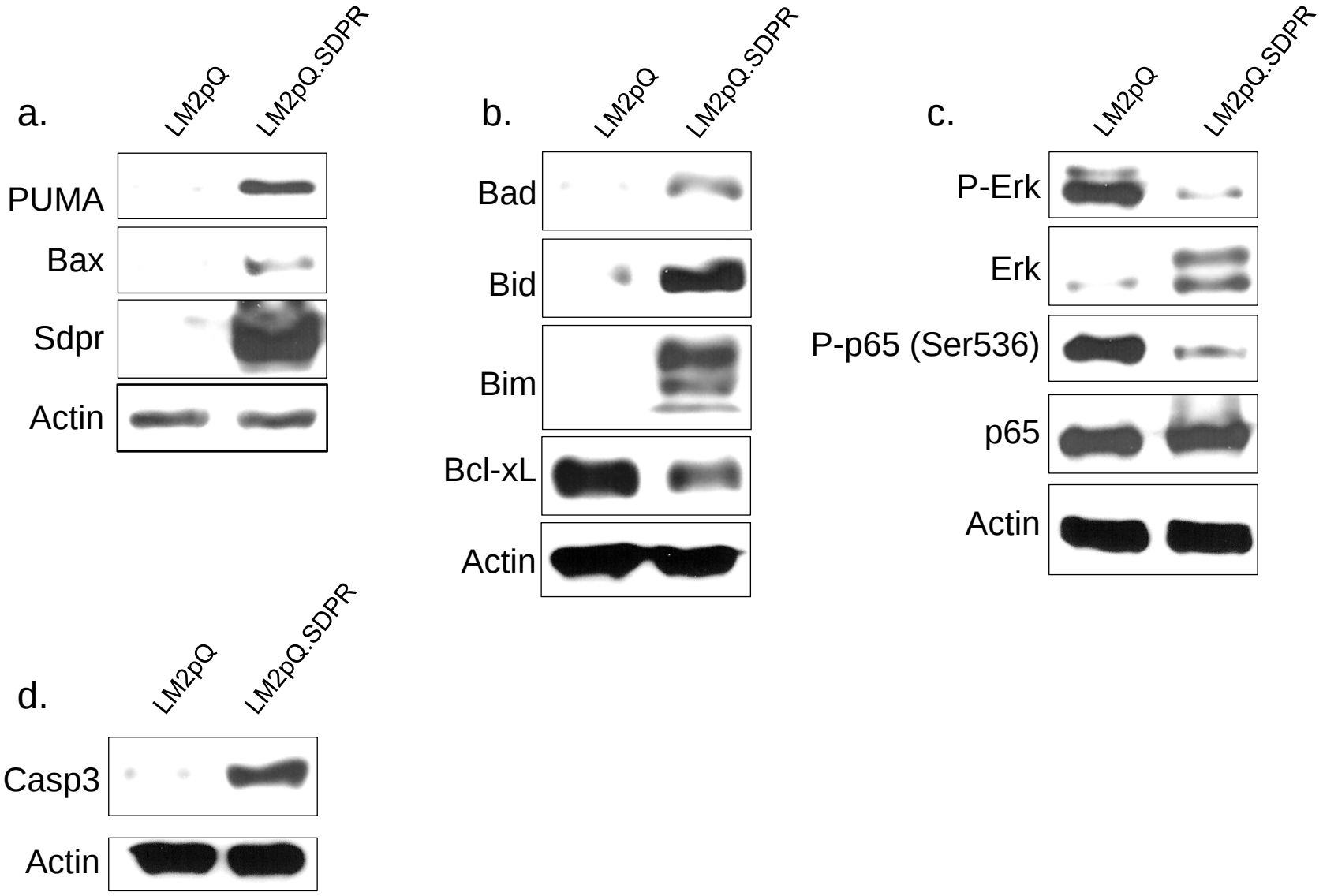

Supplementary Figure 16: SDPR primes LM2 cells for apoptosis. (a) The effects of SDPR overexpression on pro-apoptotic proteins PUMA and Bax in LM2 cells was evaluated by Western blotting. **(b)** The protein levels of Bcl-2 family members, pro-apoptotic, Bad, Bid, and Bim and anti-apoptotic Bcl-xL were determined by Western blot assays. **(c)** Activity of Erk and NF-κB pathways were assessed by phosphorylated Erk and phosphorylated p65 protein levels, respectively. **(d)** Caspase 3 protein levels following SDPR overexpression was assessed by Western blot analysis.

Supplementary Figure 17

Sait Ozturk et al.

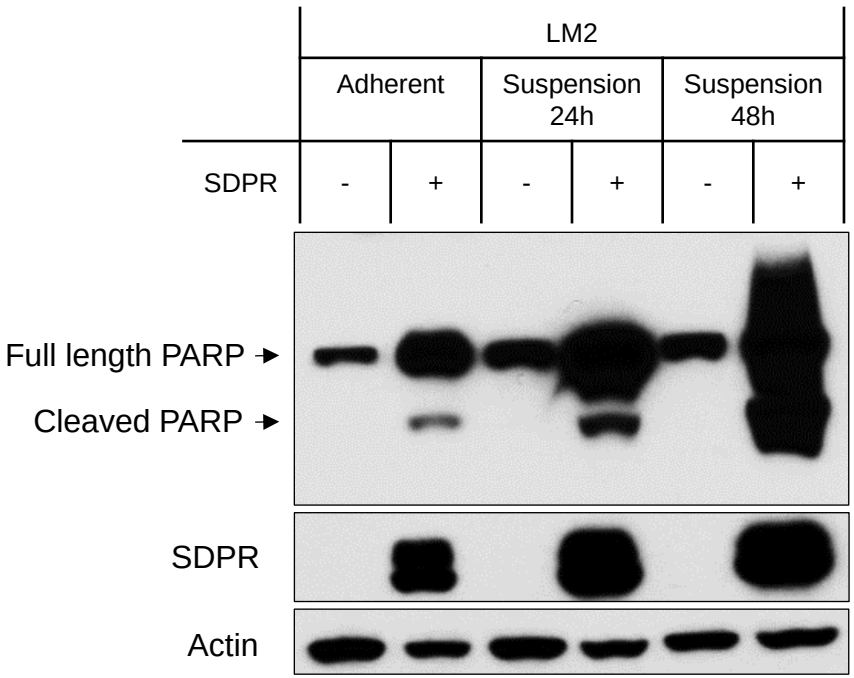

Supplementary Figure 17: Anchorage-independent growth potential of LM2 cells following SDPR overexpression. Total and cleaved PARP levels were assessed by Western blot. LM2pQ and LM2pQ.SDPR cells were grown as tumorspheres in ultra-low attachment plates for the indicated times, harvested and lysed for Western blotting.

Supplementary Figure 18

Sait Ozturk et al.

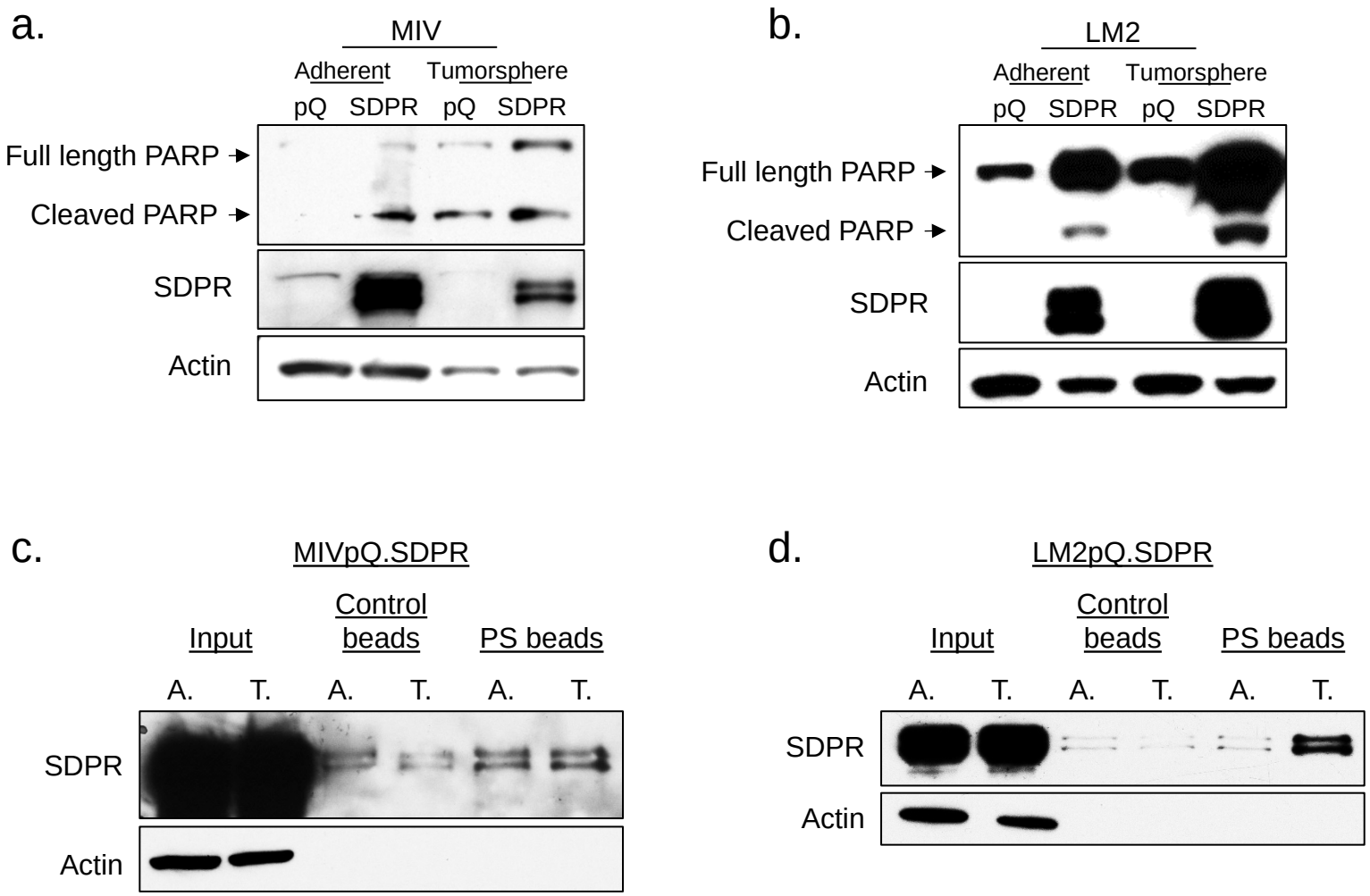

Supplementary Figure 18: SDPR interaction with phosphatidylserine (PS) during apoptosis. (a) MIVpQ and MIVpQSDPR cells were grown on plastic or as tumorspheres and cleaved PARP levels were monitored by Western blot. (b) LM2pQ and LM2pQSDPR cells were grown on plastic or as tumorspheres and cleaved PARP levels were monitored by Western blot. (c) SDPR-PS interactions in adherent versus tumorsphere MIVpQSDPR cells were assessed by utilizing PS beads and Western blotting. (d) SDPR-PS interactions in adherent versus tumorsphere LM2pQSDPR cells were assessed by utilizing PS beads and Western blotting. A.: Adherent, T.: Tumorsphere.

Supplementary Figure 19

Sait Ozturk et al.

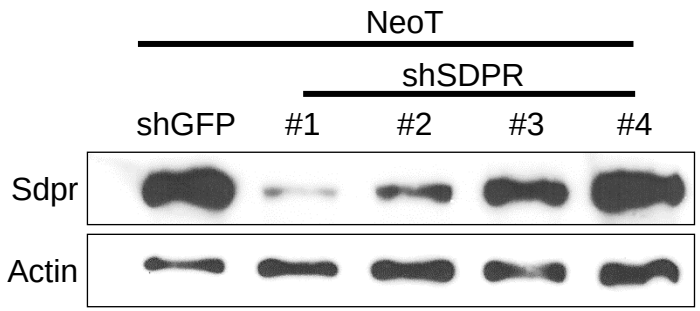

Supplementary Figure 19: SDPR knockdown in NeoT cells. SDPR was knocked down in non-metastatic NeoT cells using four different shSDPR constructs. The most complete knockdown was achieved by construct #1; hence it was used in the subsequent experiments that were performed.

Supplementary Figure 20

Sait Ozturk et al.

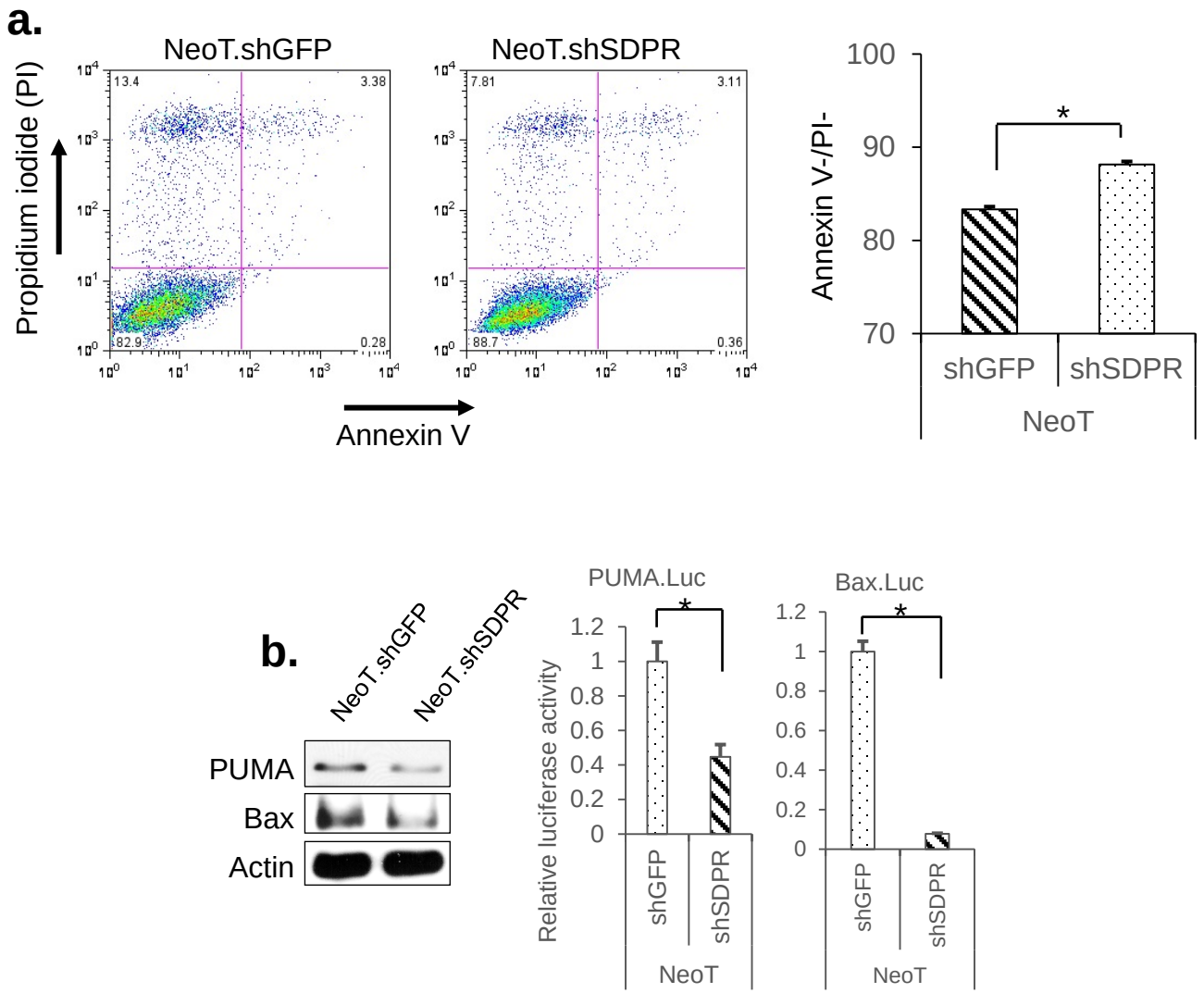

Supplementary Figure 20: Loss of SDPR increases cell survival. (a) The effect of SDPR knockdown on surviving cell population in the non-metastatic NeoT cells was measured by Annexin V staining and propidium iodide staining (quantification of three independent experiments is shown), p= 0.0065. **(b)** The effects of SDPR knockdown on the pro-apoptotic PUMA and Bax expression in NeoT cells was evaluated by western blotting and luciferase reporter assays. The p-values for luciferase reporter assays were: p_{PUMA}=0.0014, p_{Bax}= 0.0016. * indicates P<0.05.

Supplementary Figure 21

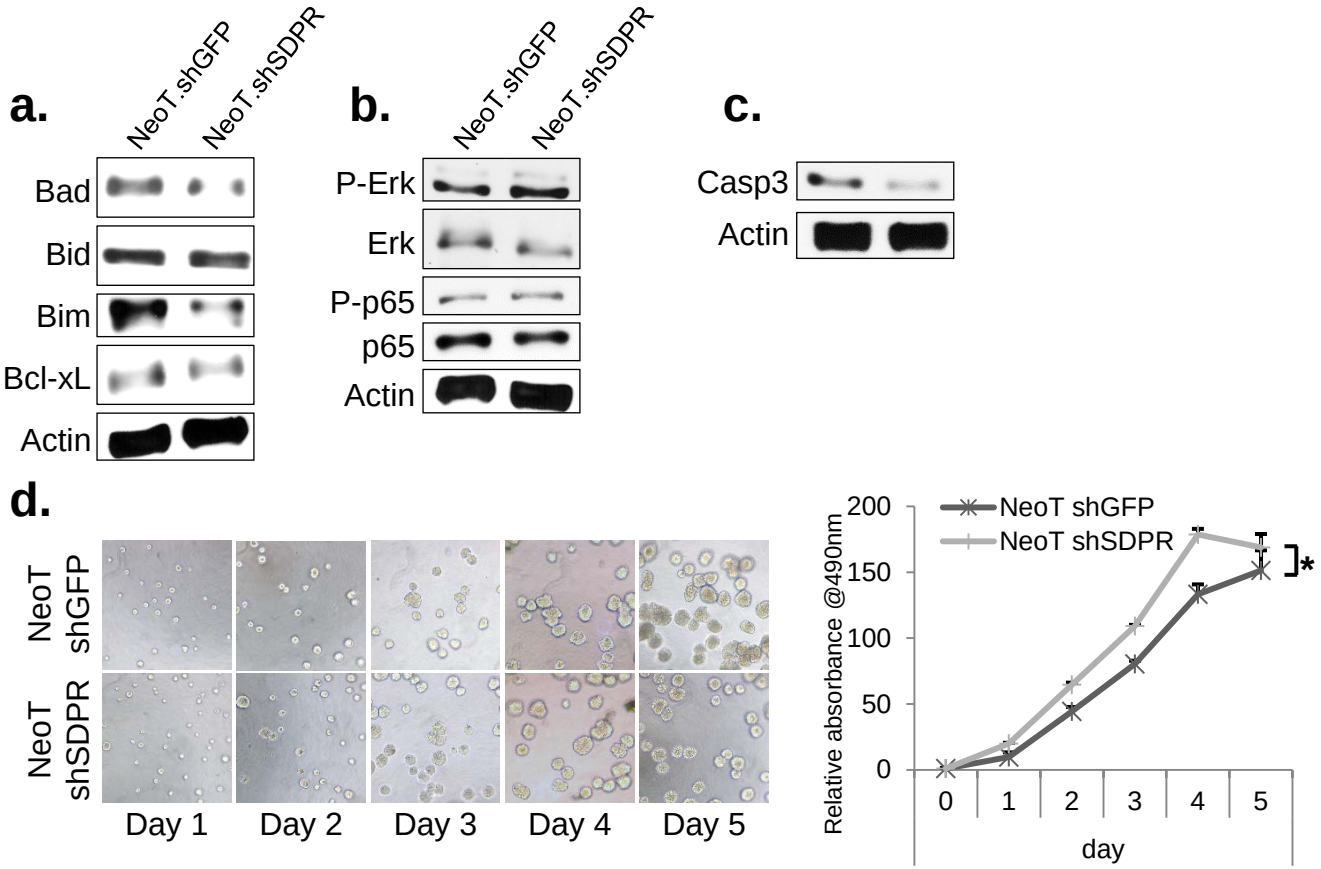

Supplementary Figure 21: Effect of SDPR knockdown on apoptosis regulators and survival following loss of cell adhesion in NeoT cells. (a) Protein levels of pro-apoptotic Bcl2 family members, Bad, Bid and Bim, and anti-apoptotic Bcl-xL were measured by Western blotting in control and NeoTshSDPR. **(b)** The activity of ERK and NF-κB pathways was assessed by Western blotting following SDPR knockdown in NeoT cells. **(c)** Total caspase 3 protein levels in control and NeoTshSDPR cells were measured by Western blotting. **(d)** Control and NeoTshSDPR cells were grown in 3D cell culture, p=0.0211, n=3.

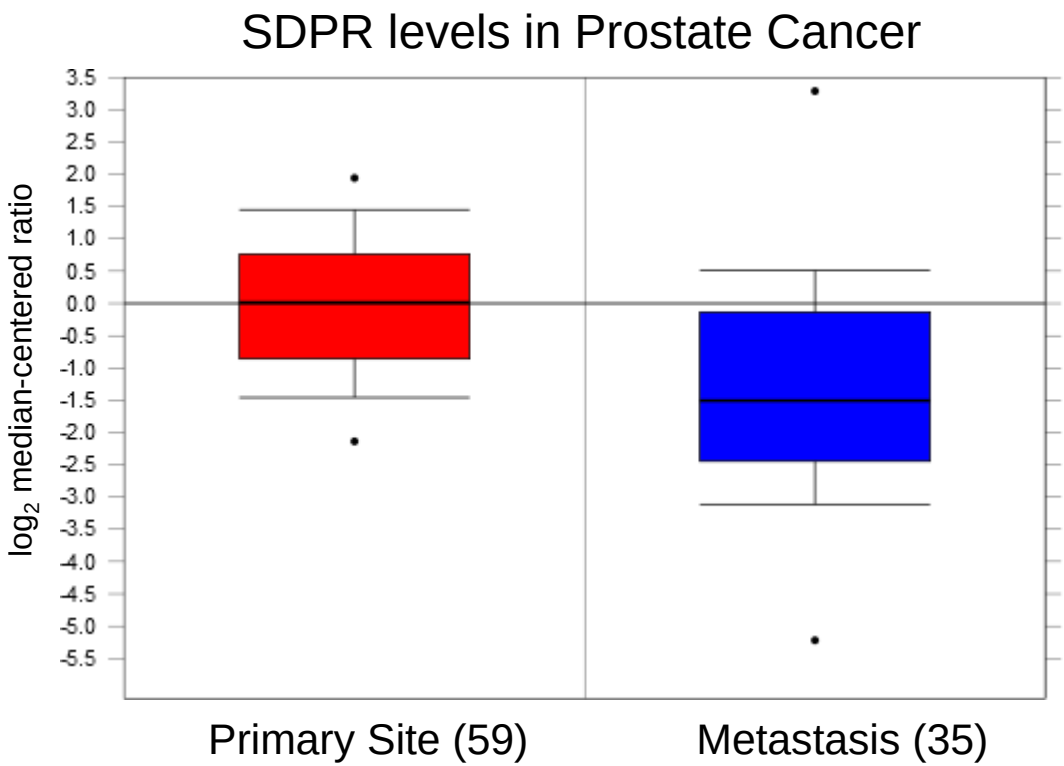

Supplementary Figure 22: Expression of SDPR in prostate cancer. Analysis on Oncomine™ database demonstrated a significant downregulation of SDPR during prostate cancer progression, *p*=1.73E-5 and numbers in parenthesis indicate the sample sizes.

Supplementary Figure 23

Sait Ozturk et al.

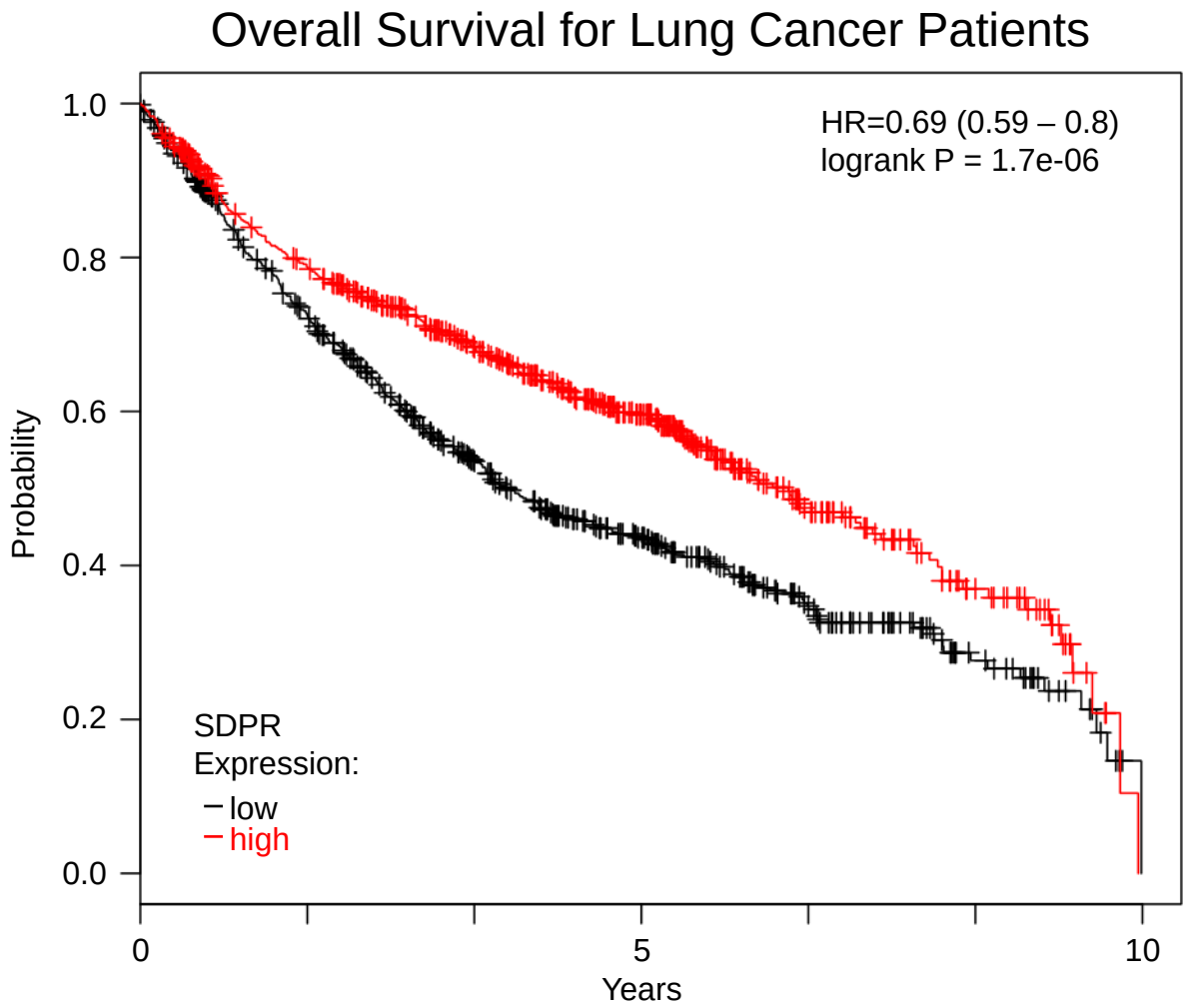

Supplementary Figure 23: SDPR expression and lung cancer prognosis. *In silico* Kaplan-Meier analysis indicated an association between SDPR expression and overall survival. The analysis run on a cohort with 1337 lung cancer patients, p=1.7e-06.

Supplementary Figure 24

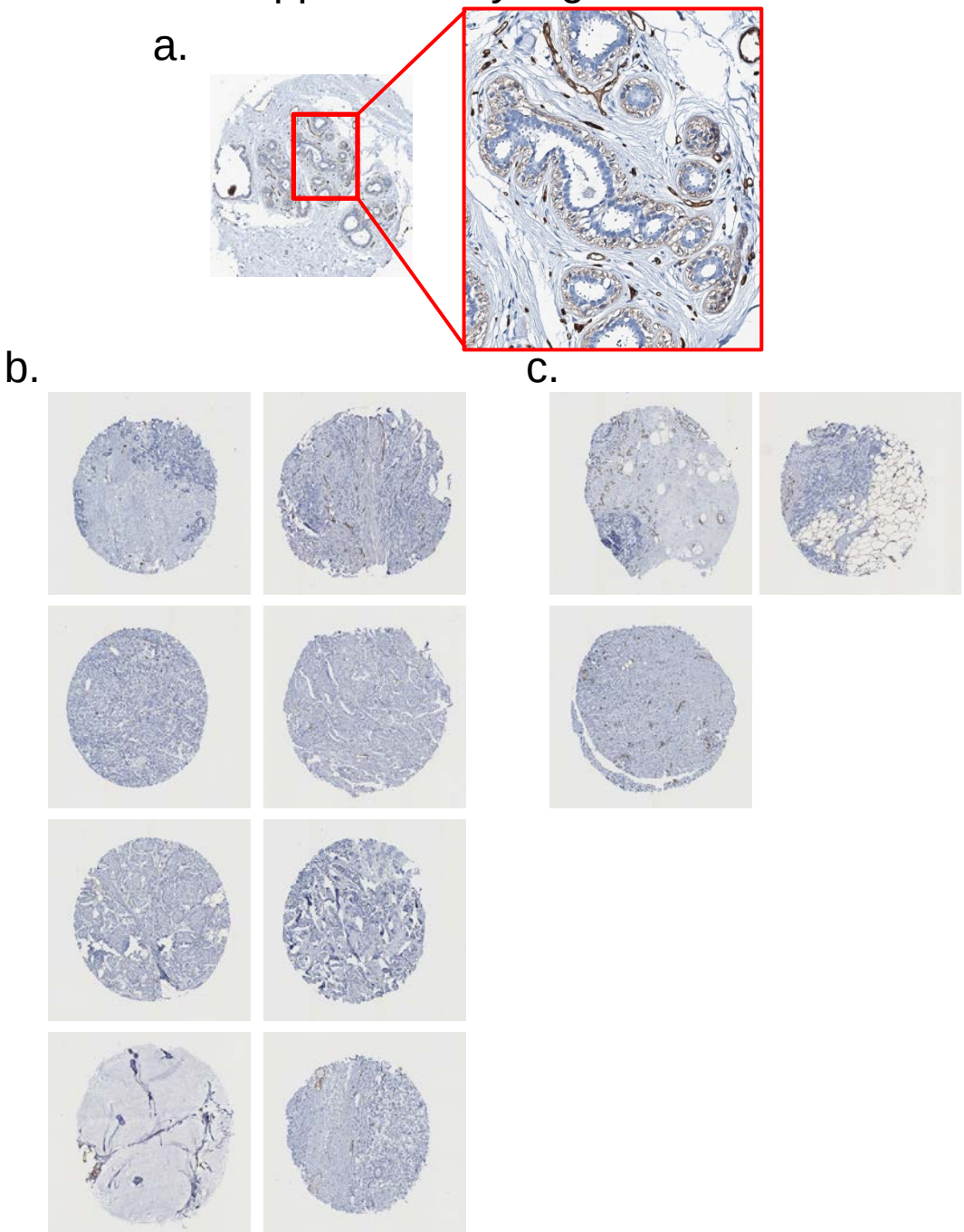

Supplementary Figure 24: The Human Protein Atlas database reveals loss of SDPR protein in breast cancer. **(a)** Myoepithelial cells in normal breast tissue were positive for SDPR protein. On the other hand, ductal carcinoma samples from eight patients **(b)** and lobular carcinoma samples from three patients **(c)** were all negative for SDPR protein staining.

Supplementary Figure 25

Sait Ozturk et al.

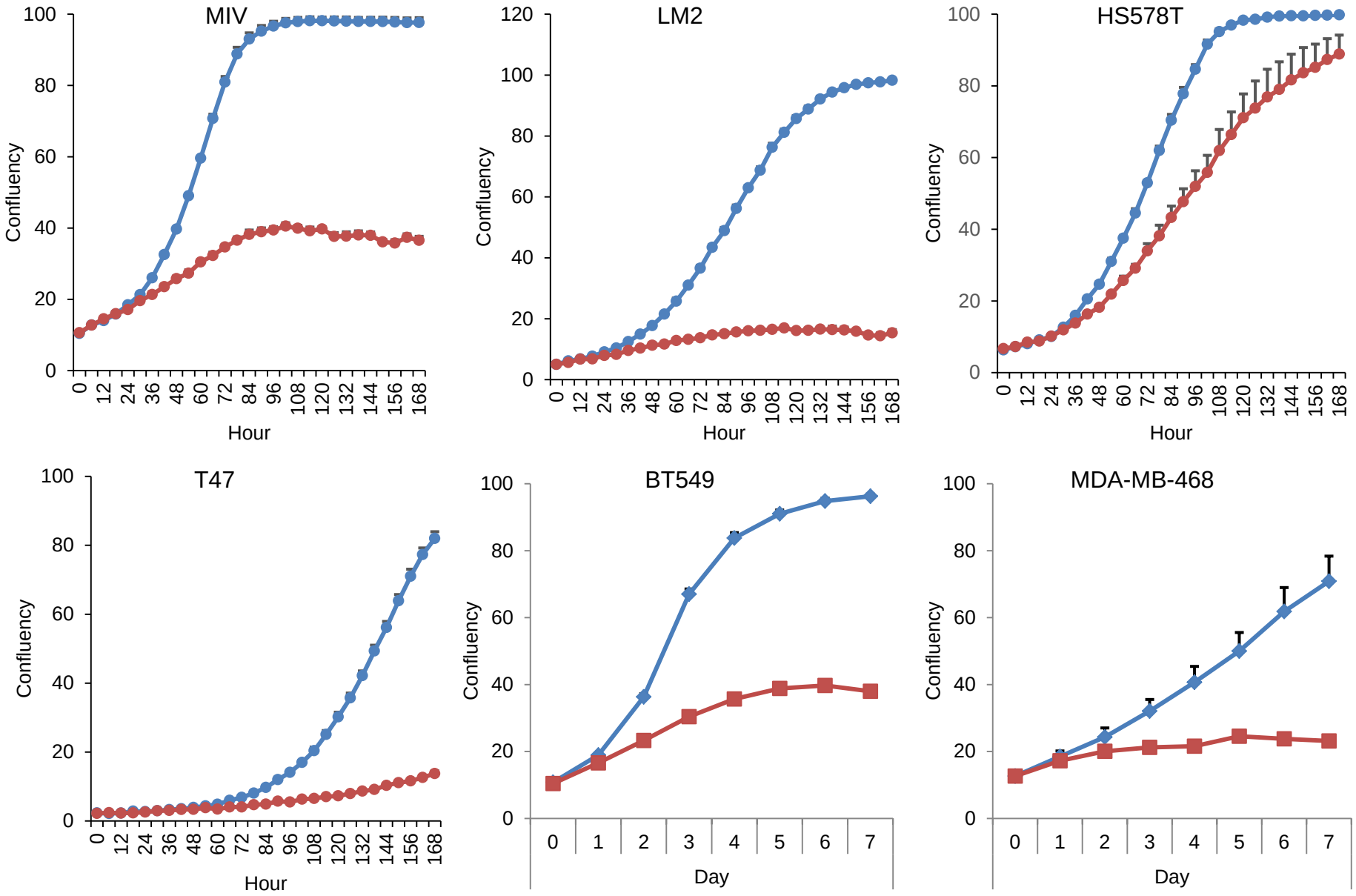

Supplementary Figure 25: Effect of 5-aza treatment on growth of metastatic breast cancer cell lines. Cells were mock treated (blue curves for each cell line) or treated with 5μM 5-aza (red curves for each cell line) and growth was measured by IncuCyte ZOOM® Live Cell Imaging system. The confluency of the cells in each well was assessed using the software based on whole well light microscopy pictures.

Supplementary Table 1
File lists the candidate metastasis suppressor genes after Oncomine™ analysis and the primers used in quantitative RT-PCR.

	Cluster 7	
	Forward	Reverse
SLPI	AGGCTCTGGAAAGTCCTTCA	TCTGGCACTCAGGTTTCTTG
LPL	CAGCCAGGATGTAACATTGG	CTCGTGGGAGCACTTCACTA
PLLP	CAAGCAACACGTAGCACCTT	GAGAGGTTGGTTGAAACGGT
KRT6A	GGGTGTGATCTCACTGTTGG	AGTCCTGGAAGGTGAGCTTG
KLF4	GGCACTACCGTAAACACACG	CTGGCAGTGTGGGTCATATC
MIA	ATTGTCCGAGAGGACCAGAC	CACTGGCAGTAGAAATCCCA
CYP1A1	AAACCCAGCTGACTTCATCC	TGCTCCTTGACCATCTTCTG
ACAT2	GCCTTGCAGTCCAGTCAATA	TAAGCCAAGTGAGGAGCCTT
PDZD2	CCACAGGAAACCCTTGATCT	TGTGGTGTTTCTGTCAGGGT
KRT14	ATTGAGAGCCTGAAGGAGGA	ATTGACATCTCCACCCACCT
SCNN1B	CCAGAGCTTGTGTCCTTCAA	GGGTAGGAACCAGGTGAAGA
AQP3	CAGTGGGACGTGTTTCTGTC	CCCGGATCCCTAAGACTGTA
DEFB1	TCATTACAATTGCGTCAGCA	TTCTGCGTCATTTCTTCTGG
PLAC8	GCAACTCTTTGCTGTCCTCA	AAAGTACGCATGGCTCTCCT
ZNF365	ATTCCGACAGGGTGTCTTTC	AAAGAAGACGGCAGAGGTGT
S100A4	TTCTTGGTTTGGTGCTTCTG	AGCAGTCAGGATCAACACGTA
ZNF44	GGCCCTGTGTTATGGAACTT	GATATCCACTAGGCCCTCCA
GJA5	ACTGACAGGCTCAAGAGCAA	TTCTTCACACTCTGGCTGCT
PCSK5	GGTGACTGGGTCCTTGAAGT	GTTGGTGAATATGGCTGCAC
CDA	GCAGGCAAGTCATGAGAGAG	CATTCTCTGGCTGTCACTGG
GABRA2	TTCGCCTCCTTCTACACCTC	ACTGCAGCAGCCAAGAGAG
CORO2A	TTGAAATTTGAGAAGGGCAA	TCCAGGAGCTCCACCTAAAT
DHRS9	TTGCTCCATCTACCAGAACAA	AAAGCGGACAGACAAACAGA
LYPD3	CAACCAGTCAGACTCCGAGA	GGATACTGCCCTGAATTGCT
ARL4D	AGAAGAGACGGTGACCCAAG	TCCTTCATTGAGGTGGACAG

	Cluster 6	
	Forward	Reverse
SSBP3	TCCCACCCCTTGCCCTTTCC	GGTGGAAGGGCTTGGGCACA
MYADM	GTGCACTTTCGCTGGGTTCCGT	GGGGGAGGTAGGCCGTTAGC
ZNF302	GACGGTGAGGCCCTGCTGAG	TGGTTGAAGGCTGCCCCACT
SLC14A1	CCTTGTCGTGGAGGTGGGCAAAT	GCCGCCAATCAAAGACCGTCC
MYLIP	CCGGACAAGGGTCCGCAGAG	GCGTCCGGCCTCGTCACATA
DHRS9	TCATACCAGAAGGAGCACCCACCT	AGACCCAACAAGAGGTCCTGCG
SCNN1G	GGCCCAGAGCCCTTGGAGTG	CCCAGAGCATGGCCCACCAT
FKBP1B	GGCCAAACGTGTGTGGTGCA	CCCCAAGCTCATCTGGGCTG
HIST1H2BD	TTGCCAAGGGAGAGACATGAAGACA	ACCAGTGTGCAGCAAACCAGGAT
SEPP1	TCAGAGTGTGCTGCTGTGGCTT	CTCCACATTGCTGGGGTTGTCACA
AOX1	GGTGCCCGCTACTTCCCAGAAC	CACCTTGCGGCCGTTCACGT
SORBS2	TGATCACAGCCACGCAGGCC	CAGTCCAGTGCCCGTCCCAG
SDPR	AGTCACGGTGCTCACGCTCC	GTTGCTGGTGGAGGCCTGGT

BIN1	TTTCGCGGCTGCGCAGAAAG	AGGCCTCTGCTGGCTGAGATG
EFEMP1	AAGGCGTGGAAATGCCACTTTGAG	CCTGTGACTTGACCAGCGCCA
MT1E	TTCCAACTGCCTGACTGCTTGTTCG	CTCTTTGCACTTGCAGGAGCCG
SGK1	ACGTCTTTCTGTCTCCCCGCGG	ACCATGCCCCTCATCCTGGAGT
CDH19	GCGGGAACGCAAGACTCGGA	GGCACTGTCGGGGCCAACTT
LIMCH1	CATCCCGGCGCTTGAGAGGA	TTCTGCGCCTCGGAGAAGGC
TACC1	CTTCCCGGCTAGTGGAGCCC	CCCCAGGTCCTGCCAATCCG
KLF9	ACGCCCTTGTGATTGGCCGA	ACGTTCCAGCTTGCGGAGCT
BCL11B	CCCACCCTCACTCATCCGTGATCA	AGGGCTGCTTGCATGTTGTGC
LPCAT2	TCGCTTCGGCCGGGTTCTAC	ACAATCTGGACCCGCCTCGC
TFPI	CAAGGCGGATGATGGCCCATGT	ACGACACAATCCTCTGTCTGCTGG
HOPX	TCCCCGTCTTCTCTCAGCCACA	GCAGCGTGGGCAGGAGGTAA
GNG2	CTGTCGTGGAGGTGACCGTGG	GCTCCTGGGCTGCTGACAGT
TIMP3	GCTCTCAGCTCTCGGGCCAG	TGTCTCCTGGGGGCCACAGT
RHOBTB3	GCTCCTTTGTGTCCAGCCGC	CAGCTGACCGCAGTCCCCTC

Supplementary Table 2

Sait Ozturk et al., 2015

Type	Number of studies that showed significant **downregulation** of SDPR	Number of studies that showed significant **upregulation** of SDPR
Bladder Cancer	1	0
Breast Cancer	12	0
Colorectal Cancer	2	0
Lung Cancer	5	0
Pancreatic Cancer	1	0
Ovarian Cancer	1	0
Other	1	0
Sarcoma	4	0
Brain and CNS cancer	0	1
Total	27	1

Search parameters:

Threshold (Gene Rank): Top 1% Threshold (Fold Change) 2 Threshold (P-value): 1E-4

Oncomine™ (Compendia Bioscience, Ann Arbor, MI) was used for analysis and visualization.

Supplementary Table and Data Legends:

Supplementary Data 1: Hierarchical clustering of differentially expressed genes among model breast cancer cell lines. The heat map reveals that there are 12 distinct gene clusters among the MII, MIII and MIV cell lines. Among these 12, cluster 6 and 7 were hypothesized to harbor metastasis suppressor genes.

Supplementary Table 1: List of candidate metastasis suppressor genes selected after Oncomine™ analysis. We observed 51 genes that are suppressed in cancer samples according to meta-analysis of the Oncomine™ database. The list also includes the primers used in quantitative RT-PCR for each candidate gene.

Supplementary Table 2: Summary of Oncomine™ analysis for *SDPR*. Oncomine™ database analysis shows that SDPR is significantly suppressed in a wide variety of cancer types in 27 separate studies (1-13).

Supplementary Methods

Cloning: We amplified the *SDPR* coding region by using the following primer pair:

F: 5’ GAGA GCGGCCGC ATG GGAGAGGACGCTGCACAGGCCGAAAAGTTCCAGC 3’

R: 5’ GAGA TTAATTAA TCA GTGGTGATGGTGATGATG GGAGGTCTGGTGCACC 3’

Filler Sequence, Restriction Sites, Start/Stop Codons, 6-His Tag, SDPR specific sequence

Template cDNA was synthesized using total RNA isolated from MII cells and cloned into pQCXIP retroviral expression vector. The correct SDPR sequence was confirmed by sequencing, and expression was confirmed by western blotting.

We used the following four oligos to target SDPR for knockdown using pLKO.1 lentiviral plasmid:

#1: 5’-GCAGTGAGCAGATGCCAAATG-3’

#2: 5’-GGCACAGAAGGTACGCTATGA-3’

#3: 5’-GCATCCAGAATGACCTCACCA-3’

#4: 5’-CCAGCCTGAAGAAGTGGATAGCCTCAAG-3’

Statistical analysis: For growth curve comparisons, Analysis of Variance (ANOVA) test was used. For all other experiments, *p*-values were calculated by one tailed, t-test. *p*-values smaller than 0.05 were considered significant. In all experiments error bars represent standard error. All experiments were performed in triplicates unless a different sample size is noted.

Methylation specific quantitative PCR:

Primer sequences were as follows:

Methylated-specific forward: 5'-TCGGGATAATTTATAGGTGAACGT -3'

Methylated-specific reverse: 5'-AAATCATTCTAAATACCCTTCACGA -3'

Unmethylated-specific forward: 5'-TTTGGGATAATTTATAGGTGAATGT-3'

Unmethylated-specific reverse: 5'-AATCATTCTAAATACCCTTCACAAA-3'

Drug treatments: Cells were grown in complete medium overnight prior to treatment with 5 μmol/L 5'-aza-deoxycytidine for 72 hours.

Coimmunoprecipitation assays: For each conditions, 2x15cm plates were lysed in 1.5ml/plate ice cold BC-200 buffer (1mM EDTA, 25mM Tris -ph 7.5, 0.2% Triton-X, 200mM KCl, 10% Glycerol (vol/vol) with protease and phosphatase inhibitors) in a cold room on a shaker for 15 minutes. Following the 15 min incubations, lysates were collected and kept on ice for 10 minutes during which time the samples were vortexed twice for 10 seconds. Then, samples were centrifuged at 20,000g at 4°C for 20 min and supernatants collected for immunoprecipitation. Magnetic Dynabeads® were equilibrated by washing them once with BC-200 buffer. HIS AB from Cell Signaling (Cat #2366) or for control mouse IgG was bound to Dynabeads through 2 hour incubation in the cold room. Meanwhile, cell lysates were pre-cleared by incubation with Dynabeads in the cold room for 2 hours. Following AB binding and pre-clearing, Co-IP was performed by adding pre-cleared lysates to HIS AB or IgG bound Dynabeads for 4 hours in the cold room. Dynabeads were washed 5 times with BC-200 buffer and then boiled with SDS sample buffer followed by separation with SDS-PAGE.

Cell proliferation assay: Five thousand cells per well were seeded in 96-well plates and the number of cells assessed daily for five days using the MTS tetrazolium/PMS assay kit (Promega,

Madison, WI) according to the manufacturer's protocol and the absorbance at 490nm recorded by Bio-Tek µQuant plate reader.

To assess the growth of cells following 5-aza treatment, we seeded five thousand cells in 96-well plates and monitored the growth of control and 5µM 5-aza treated cells for 7 days by using IncuCyte ZOOM® Live Cell Imaging system (Essen BioScience) which consist of a microscope gantry. The confluency of the cells in each well was assessed by the software based on whole well light microscopy pictures.

Cell migration assays: For the scratch wound healing assay, cells were grown to confluency and a scratch wound created with a 200 µl pipette tip. The rate of wound closure was monitored by light microscopy at 0 and 20 hours.

The Boyden chamber assay was performed using 6-well Transwell plates with an 8 µm pore (Corning, Tewksbury, MA). One hundred thousand cells were seeded on the upper compartment of the chamber in serum-free DMEM/F12 medium and allowed to migrate towards either serum-free or complete medium for 20 hours. The top side of the membrane was then cleaned with cotton swabs and the migrated cells stained with 0.5% crystal violet solution and visualized by light microscopy.

Trans-endothelial migration assay: HUVEC cells were seeded on fibronectin (Sigma, St. Louis, MO) coated Transwell inserts and grown into a barrier of monolayer cells. 10^5 breast cancer cells were serum-starved overnight, harvested, and seeded on top of the HUVECs in serum-free medium for 48 hours while the receiver plate is filled with complete medium to serve as chemoattractant. Breast cancer cells that migrated through the endothelial cell layer (Transendothelial migration) from the apical to the basal side of the inserts are dissociated with Cell Dissociation Buffer (Life Technologies, Carlsbad, CA) onto a new 6-well receiver plate and

stained with Calcein AM (Life Technologies, Carlsbad, CA). The relative amount of migrated breast cancer cells (pQ vs pQSDPR) is then determined using a fluorescent plate reader at 485nm excitation and 520nm emission.

Cell culture: MCF-10A based cell lines, which include NeoT, MII, MIII, MIV, MIVpQ, MIVpQ.SDPR, NeoTshGFP and NeoTshSDPR, were cultured in DMEM/F12 1:1 mixture medium supplemented with 5% horse serum (vol/vol), 1% penicillin/streptomycin solution (vol/vol), 10 µg/ml insulin, 0.1 µg/ml cholera toxin, 20 ng/ml epidermal growth factor and 0.5 µg/ml hydroxycortisone. MDA-MB-231LM2 cells were cultured in DMEM medium supplemented with 10% FBS (vol/vol) and 1% penicillin/streptomycin solution (vol/vol). Human Umbilical Vein Endothelial Cells (HUVEC) cells were cultured in Endothelial Cell Medium from Sciencell supplemented with 25 ml fetal bovine serum and 5 ml of endothelial cell growth supplement for 500 ml of total media.

Tumorsphere assays: For tumorsphere assays, cells were grown in ultra low attachment plates (Corning, Teterboro, NJ) using DMEM (for LM2) or DMEM/F12 (for MIV) media (Thermo Fisher Scientific, Waltham, MA) containing 20ng/ml FGF (R&D Systems, Minneapolis, MN), 20ng/ml EGF (PeproTech, Rocky Hill, NJ), 2% B27 supplement (vol/vol) (Thermo Fisher Scientific, Waltham, MA) and 1% P/S (vol/vol) (Thermo Fisher Scientific, Waltham, MA).

Phosphatidylserine affinity assays: For PS affinity assays, PS beads and the accompanying control beads were acquired from Echelon, San Jose, CA. Cells were grown on plastic or as tumorspheres for 24 hours and harvested using lysis buffer (10mM HEPES at pH 7.4, 150mM NaCl and 0.25% Igepal). After vortexing, lysates were sonicated 3 seconds 3 times. Following sonication, centrifugation at 20,000g was taken place for 30min. Control and PS beads were equilibrated in lysis buffer. Beads were incubated with lysates overnight with a rotator. Next day,

beads were washed with lysis buffer 4 times and PS-interacting proteins were eluted by 2X Laemmli sample buffer.

Luciferase reporter assays: Transient transfection of reporter constructs (luciferase gene driven by PUMA and Bax promoters were generous gifts from Drs. Bert Vogelstein and Jian Yu, Howard Hughes Medical Institute at Johns Hopkins) were performed using FuGENE transfection reagent (Roche) following the manufacturer's protocol. As a transfection control, Renilla luciferase was co-transfected with the reporter constructs. After 48 hours of transfection, cells were lysed in Passive Lysis Buffer (Promega, Dual-Luciferase Reporter Assay) and luciferase activity was measured at 570 nm. Subsequent to the reaction termination, Renilla luciferase activity was measured as an internal control. Renilla/Firefly Luciferase ratio was used to compare activity of reporter constructs in different samples.

Antibodies: Anti-SDPR antibodies were obtained from Sigma (St. Louis, MO). Antibodies against PUMA, Bax, Bad, Bid, Bim, Bcl-xL, total Erk, phosphorylated Erk (Thr202/Tyr204), total p65, phosphorylated p65 (Ser536), total and cleaved Casp3 were obtained from Cell Signaling (Danvers, MA). Anti-beta Actin antibody was obtained from Abcam (Cambridge, UK). Anti-HIS-tag antibody was obtained from Roche (Basel, Switzerland).

***In vivo* metastasis and tumorigenicity assays:** For *in vivo* metastasis assays involving MIV based cell lines, $5x10^5$ cells were injected through the tail vein, and animals were monitored by bioluminescent imaging for 11 weeks. For the *in vivo* metastasis assays involving LM2 based cell lines, $1x10^6$ cells were injected through the tail vein, and animals were monitored for 7 weeks. Prior to imaging, animals were injected with D-luciferin (150mg/kg - intraperitoneal). In vivo tumorigenicity assays were done by subcutaneously injecting 5x105 MIV cells. Animals

were monitored for 5 weeks by bioluminescent imaging and tumor sizes assessed at the end of the experiment by measurement of tumor weight.

References:

1. Sanchez-Carbayo M, Socci ND, Lozano J, Saint F, & Cordon-Cardo C (2006) Defining molecular profiles of poor outcome in patients with invasive bladder cancer using oligonucleotide microarrays. *Journal of clinical oncology : official journal of the American Society of Clinical Oncology* 24(5):778-789.
2. Ki DH*, et al.* (2007) Whole genome analysis for liver metastasis gene signatures in colorectal cancer. *International journal of cancer. Journal international du cancer* 121(9):2005-2012.
3. Sabates-Bellver J*, et al.* (2007) Transcriptome profile of human colorectal adenomas. *Molecular cancer research : MCR* 5(12):1263-1275.
4. Garber ME*, et al.* (2001) Diversity of gene expression in adenocarcinoma of the lung. *Proceedings of the National Academy of Sciences of the United States of America* 98(24):13784-13789.
5. Okayama H*, et al.* (2012) Identification of genes upregulated in ALK-positive and EGFR/KRAS/ALK-negative lung adenocarcinomas. *Cancer research* 72(1):100-111.
6. Selamat SA*, et al.* (2012) Genome-scale analysis of DNA methylation in lung adenocarcinoma and integration with mRNA expression. *Genome research* 22(7):1197-1211.
7. Wachi S, Yoneda K, & Wu R (2005) Interactome-transcriptome analysis reveals the high centrality of genes differentially expressed in lung cancer tissues. *Bioinformatics* 21(23):4205-4208.
8. Yoshihara K*, et al.* (2009) Gene expression profiling of advanced-stage serous ovarian cancers distinguishes novel subclasses and implicates ZEB2 in tumor progression and prognosis. *Cancer science* 100(8):1421-1428.
9. Pei H*, et al.* (2009) FKBP51 affects cancer cell response to chemotherapy by negatively regulating Akt. *Cancer cell* 16(3):259-266.
10. Barretina J*, et al.* (2010) Subtype-specific genomic alterations define new targets for soft-tissue sarcoma therapy. *Nature genetics* 42(8):715-721.
11. TCGA (2011) (The Cancer Genome Atlas) - Invasive Breast Carcinoma Gene Expression Data. *Office of Cancer Genomics, National Cancer Institute, National Institutes of Health, Bethesda, MD 20892.*
12. Curtis C*, et al.* (2012) The genomic and transcriptomic architecture of 2,000 breast tumours reveals novel subgroups. *Nature* 486(7403):346-352.
13. Ma XJ, Dahiya S, Richardson E, Erlander M, & Sgroi DC (2009) Gene expression profiling of the tumor microenvironment during breast cancer progression. *Breast cancer research : BCR* 11(1):R7.